Direct Fractional-Order Adaptive Control Design for Cascaded Doubly-Fed Induction Generator (CDFIG) in a Wind Energy System

SIHEM DJEBBRI[1], SAMIR LADACI[2,*]
[1]Department of Electrical Engineering,
20 August 1955 University,
Elhadaiek, Skikda 21000,
ALGERIA

[2]Department of Automatic Control Engineering,
Ecole Nationale Polytechnique,
El Harrach, 16200, Algiers,
ALGERIA

[*]*Corresponding Author*

Abstract: - This paper is devoted to a fractional-order model reference adaptive control (FO-MRAC) synthesis for the independent control of the active and reactive power flows in the cascaded doubly fed induction generator (CDFIG) in wind energy systems. The proposed adaptive control law combines a second-order-like fractional reference model and a direct MIT adaptation law using a fractional order integrator. This generator configuration can be an interesting alternative to standard double-output wound rotor induction generators. It is made up of two identical wound rotor induction motors such that their rotors are mechanically and electrically coupled. Using two cascaded induction machines permits the elimination of the brushes and copper rings in the traditional doubly-fed induction generator DFIG, which makes the system more resistant and reduces maintenance costs. In the first step, we propose a classical PI controller synthesis to regulate the active and reactive power produced by CDFIG. Then, the FO-MRAC design is realized and a comparative study based on numerical simulations is performed between the classical regulators PI, MRAC, and FO- MRAC, to demonstrate the superiority of the proposed fractional-order adaptive controller relative to conventional integer order PI and MRAC controllers. These results illustrate the reliability and efficiency of the proposed adaptive control scheme.

Key-Words: - MRAC, FOMRAC, Direct fractional adaptive control, Cascaded Doubly Fed Induction Generators, Variable Speed Generator, Active-Power, Reactive Power, Wind Energy System.

Received: April 5, 2024. Revised: August 21, 2024. Accepted: October 3, 2024. Published: November 5, 2024.

1 Introduction

For more than three centuries, a great number of researchers have concentrated on fractional calculus, [1]. Since its beginning in 1695, fractional calculus has established itself as one of the most productive and current branches of modern mathematics, [2].

The fields of application of these fractional operators are varied and affect practically all specialties of engineering and science.

As far as we are concerned in this work, fractional order control and its application in renewable energy systems and electrical machines have been the subjects of a sustained research effort bringing several innovations to increase efficiency and the effectiveness of these systems, [3], [4], [5], [6], [7].

Fractional adaptive control is a very recent and hot research topic, gathering more and more interest these recent years because of the improvement obtained in the control system performance when compared to the classical adaptive control schemes, [8], [9], [10], [11], [12]. The reason for this enthusiasm lies in its extraordinary simplicity to implement and its ability to augment the system's dynamic performance and robustness when compared to conventional adaptive control techniques, [13], [14].

A plethora of applications using fractional-order model reference adaptive control (FOMRAC) configurations can be found in literature, covering a wide range of science and engineering domains like Voltage control of DC/DC converter in multi-

sources renewable energy systems [15], in multi-source renewable energy system using fractional-order integrals, [16]. In the wind energy system, using adaptive control of a Doubly Fed Induction Generator (DFIG) and Cascaded Doubly-Fed Induction Generators using a fractional-order PI^{λ} controller, [17]. Recently, fractional adaptive control schemes based on fractional order identified models have been developed with interesting results, [18], [19], [20], [21], [22]. Today wind parks occupy a very considerable place in the field of the production of electrical energy, [23]. Indeed, thanks on the one hand to the sensitivity and the importance of the sector of energy production and on the other hand to the development and consequently to the various structures of the chains of production [24], [25], [26], the windmills play a dominating role to satisfy the energy needs and the economic requirements.

Wind energy systems are generally equipped with asynchronous machines with double-fed induction generators (DFIG) functioning at variable speeds, [27], [28], [29]. Unfortunately, in this structure of conversion, the presence of the system ring brushes reduces the reliability of the machine, [30]. However, with regard to this work, we propose to study the performance of windmill chains where two DFIG are coupled electrically and mechanically via their rotors, in order to improve the performances of the production chains.

Proportional-integral (PI) controllers are the most commonly used for such energy processes, unfortunately, the adjustment of controller parameters is not a simple task and usually needs a continuous correction. Besides, the parameters obtained analytically or by simulation usually fail in practice. These PI controllers can guarantee good dynamic response during nominal conditions, but they may lose their performance during the grid disturbances mainly because the stator flux is not constant [17].

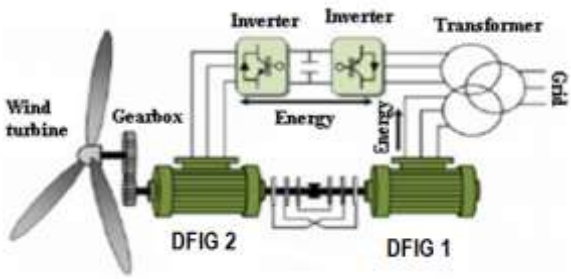

Fig. 1: CDFIG configuration for wind power generation

To compensate for these drawbacks, a design and implementation of a FOMRAC controller for the CDFIG is presented in this paper. The active and reactive power quantity is controlled in order to track permanently the maximum aerodynamic power of wind energy.

This paper presents the synthesis and implementation of a fractional order model reference adaptive control (FO-MRAC) in order to regulate the active and reactive power of a grid-connected wind turbine based on a cascade doubly fed induction generator CDFIG.

This manuscript is structured as follows: First, we introduce the Modelization of the CDFIG Generator by electric, magnetic, and power equations. Then the control systemusing a classical PI controller and the proposed fractional-order MRAC power control is defined for a CDFIG system. Then, a comparative study of simulation results is realized and discussed to show the superiority of the proposed adaptive control strategy applied to the cascaded doubly fed induction Generators CDFIG. Finally, concluding remarks are given with future research vectors on this topic.

2 Modelization of the Cascaded Doubly Fed Generator CDFIG

Thus, the structure of the chains of production is illustrated in Figure 1. The stator of the first machine is connected directly to the electrical supply network on the other hand the stator of the second machine is connected to the same network via a frequency converter that we suppose ideal, [31], [32], [33].

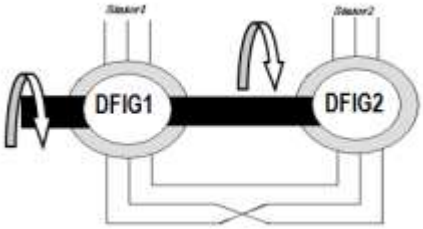

Fig. 2: Mechanical and electric connections of CDFIG

The two DFIG configurations for rotor connection are possible. Connecting the same phases results in a direct connection or reversing the two phases gives an opposite connection, [34]. In our case, is it is considered that the two rotors are connected in this last configuration illustrated in Figure 2.

In the following paragraph, we present the modelling of the CDFIG in the Park reference, and then the control of active and reactive powers transit

between the wind generator and the electrical supply network, [35].

2.1 Electric Equations

First machine:

$$\begin{cases} V_{ds1} = R_{s1}.i_{ds1} + \dfrac{d}{dt}\phi_{ds1} - \omega_s \phi_{qs1} \\ V_{qs1} = R_{s1}.i_{qs1} + \dfrac{d}{dt}\phi_{qs1} + \omega_s \phi_{ds1} \\ V_{dr1} = R_{r1}.i_{dr1} + \dfrac{d}{dt}\phi_{dr1} - (\omega_s - \omega_{r1}).\phi_{qr1} \\ V_{qr1} = R_{r1}.i_{qr1} + \dfrac{d}{dt}\phi_{qr1} + (\omega_s - \omega_{r1}).\phi_{dr1} \end{cases} \quad (1)$$

Second machine:

$$\begin{cases} V_{ds2} = R_{s2}.i_{ds2} + \dfrac{d}{dt}\phi_{ds2} - (\omega_s - \omega_{r1} - \omega_{r2}).\phi_{qs2} \\ V_{qs2} = R_{s2}.i_{qs2} + \dfrac{d}{dt}\phi_{qs2} + (\omega_s - \omega_{r1} - \omega_{r2}).\phi_{ds2} \\ V_{dr2} = R_{r2}.i_{dr2} + \dfrac{d}{dt}\phi_{dr2} - (\omega_s - \omega_{r1}).\phi_{qr2} \\ V_{qr2} = R_{r2}.i_{qr2} + \dfrac{d}{dt}\phi_{qr2} + (\omega_s - \omega_{r1}).\phi_{dr2} \end{cases} \quad (2)$$

According to the configuration of Figure 2, we can deduce the following relations:

$$\begin{cases} V_{dr1} = V_{dr2} = V_{dr} \\ V_{qr1} = V_{qr2} = V_{qr} \end{cases} \quad et \quad \begin{cases} i_{dr} = i_{dr1} = -i_{dr2} \\ i_{qr} = i_{qr1} = -i_{qr2} \end{cases} \quad (3)$$

The preceding equations can be expressed in the state space form,

$$\dot{X} = AX + BU \quad (4)$$

Where,

$$X = [i_{ds1}\ i_{qs1}\ 0\ 0\ i_{ds2}\ i_{qs2}]^T \quad (5)$$

$$U = [\frac{di_{ds1}}{dt}\ \frac{di_{qs1}}{dt}\ \frac{di_{dr}}{dt}\ \frac{di_{qr}}{dt}\ \frac{di_{ds2}}{dt}\ \frac{di_{qs2}}{dt}]^T \quad (6)$$

$$A = \begin{bmatrix} R_{s1} & -\omega_s L_{s1} & 0 & -\omega_s L_{m1} & 0 & 0 \\ \omega_s L_{s1} & R_{s1} & \omega_s L_{m1} & 0 & 0 & 0 \\ 0 & -(\omega_s - \omega_{r1})L_{m1} & (R_{r1} + R_{r2}) & -(\omega_s - \omega_{r1})(L_{r1} + L_{r2}) & 0 & (\omega_s - \omega_{r1})L_{m2} \\ (\omega_s - \omega_{r1})L_{m1} & 0 & (\omega_s - \omega_{r1})(L_{r1} + L_{r2}) & (R_{r1} + R_{r2}) & -(\omega_s - \omega_{r1})L_{m2} & 0 \\ 0 & 0 & 0 & (\omega_s - \omega_{r1} - \omega_{r2})L_{m2} & R_{s2} & -(\omega_s - \omega_{r1} - \omega_{r2})L_{s2} \\ 0 & 0 & -(\omega_s - \omega_{r1} - \omega_{r2})L_{m2} & 0 & (\omega_s - \omega_{r1} - \omega_{r2})L_{s2} & R_{s2} \end{bmatrix} \quad (7)$$

$$B = \begin{bmatrix} L_{s1} & 0 & L_{m1} & 0 & 0 & 0 \\ 0 & L_{s1} & 0 & L_{m1} & 0 & 0 \\ L_{m1} & 0 & L_{r1} + L_{r2} & 0 & -L_{m2} & 0 \\ 0 & L_{m1} & 0 & L_{r1} + L_{r2} & 0 & -L_{m2} \\ 0 & 0 & -L_{m2} & 0 & L_{s2} & 0 \\ 0 & 0 & 0 & -L_{m2} & 0 & L_{s2} \end{bmatrix} \quad (8)$$

2.2 Magnetic Equations

First machine:

$$\begin{cases} \phi_{ds1} = L_{s1}.i_{ds1} + L_{m1} i_{dr} \\ \phi_{qs1} = L_{s1}.i_{qs1} + L_{m1} i_{qr} \\ \phi_{dr1} = L_{r1}.i_{dr} + L_{m1} i_{ds1} \\ \phi_{qr1} = L_{r1}.i_{qr} + L_{m1} i_{qs1} \end{cases} \quad (9)$$

Second machine:

$$\begin{cases} \phi_{ds2} = L_{s2}.i_{ds2} - L_{m2} i_{dr} \\ \phi_{qs2} = L_{s2}.i_{qs2} - L_{m2} i_{qr} \\ \phi_{dr2} = -L_{r2}.i_{dr} + L_{m2} i_{ds2} \\ \phi_{qr2} = -L_{r2}.i_{qr} + L_{m2} i_{qs2} \end{cases} \quad (10)$$

2.3 Powers Equations

The active and reactive powers relating to the stator of the first machine and that of the second are respectively defined by the relations (11) and (12).

$$\begin{cases} P_{s1} = V_{ds1}.i_{ds1} + V_{qs1}.i_{qs1} \\ Q_{s1} = V_{qs1}.i_{ds1} - V_{ds1}.i_{qs1} \end{cases} \quad (11)$$

$$\begin{cases} P_{s2} = V_{ds2}.i_{ds2} + V_{qs2}.i_{qs2} \\ Q_{s2} = V_{qs2}.i_{ds2} - V_{ds2}.i_{qs2} \end{cases} \quad (12)$$

thus:

$$\begin{cases} P_g = P_{s1} + P_{s2} \\ Q_g = Q_{s1} + Q_{s2} \end{cases} \quad (13)$$

2.4 Mechanical Equations

The expression of the electromagnetic couple is given as:

$$C_e = P_1 L_{m1}(i_{dr}.i_{qs1} - i_{ds1}.i_{qr}) + P_2 L_{m2}(i_{dr}.i_{qs2} - i_{ds2}.i_{qr}) \quad (14)$$

With the dynamical equation:

$$J\frac{d\Omega}{dt} = C_e - C_r - f.\Omega \quad (15)$$

3 Control System Design

The CDFIG is connected to the network via its first stator while controlling the sizes of the second stator. We control the active and reactive power which transit by stator 1, not to overload stator 1 in the case where the aerodynamic power is higher than the acceptable power of stator1, which returns, in this case, to create a second way, via stator 2. We use the biphasic modelling of the machine with direct reference (dq) in order to align the axis *d*on the stator flows ϕ_s.

$$\begin{cases}\phi_{ds1}=\phi_{s1}\\ \phi_{qs1}=0\end{cases} \tag{16}$$

For the machines of great power, we can neglect the resistance of the stator, [36]. Under these conditions, we have:

$$\begin{cases}V_{ds1}=0\\ V_{qs1}=V_s=\omega_s.\phi_{s1}\end{cases} \tag{17}$$

By replacing the flow and the tension of the first stator in the whole of the equations, we will have:

$$\begin{cases}i_{dr}=C_1.i_{ds2}-C_1.\dfrac{L_{m1}.V_s}{\omega_s.L_{s1}.L_{m2}}\\ i_{qr}=C_1.i_{qs2}\end{cases} \tag{18}$$

$$\begin{cases}i_{ds1}=\dfrac{V_s}{\omega_s.L_{s1}}\left(1+\dfrac{C_1.L_{m1}^2}{L_{s1}.L_{m2}}\right)-C_1\dfrac{L_{m1}}{L_{s1}}.i_{ds2}\\ i_{qs1}=-C_1\dfrac{L_{m1}}{L_{s1}}.i_{qs2}\end{cases} \tag{19}$$

$$\begin{cases}V_{ds2}=R_{s2}.i_{ds2}+(L_{s2}-C_1L_{m2})\dfrac{di_{ds2}}{dt}-s.\omega_s(L_{s2}-C_1L_{m2}).i_{qs2}\\ V_{qs2}=R_{s2}.i_{qs2}+(L_{s2}-C_1L_{m2})\dfrac{di_{qs2}}{dt}+s.\omega_s(L_{s2}-C_1L_{m2}).i_{ds2}+C_1.s.\dfrac{L_{m1}.V_s}{L_{s1}}\end{cases} \tag{20}$$

$$\begin{cases}P_{s1}=-C_1.V_s.\dfrac{L_{m1}}{L_{s1}}.i_{qs2}\\ Q_{s1}=\dfrac{V_s^2}{\omega_s.L_{s1}}\left(1+\dfrac{C_1.L_{m1}^2}{L_{s1}.L_{m2}}\right)-C_1.V_s\dfrac{L_{m1}}{L_{s1}}.i_{ds2}\end{cases} \tag{21}$$

Where,

$$C_1=\frac{L_{m2}}{L_{r1}+L_{r2}-\dfrac{L_{m1}^2}{L_{s1}}} \tag{22}$$

With,

$$s=s_1.s_2=\frac{\omega_s-\omega_{r1}-\omega_{r2}}{\omega_s}=\frac{\omega_s-(P_1+P_2)\Omega_r}{\omega_s} \tag{23}$$

and,

$$s_1=\frac{\omega_s-P_1.\Omega_r}{\omega_s}\quad,\quad s_2=\frac{s_1\omega_s-P_2.\Omega_r}{s_1.\omega_s}$$

3.1 PI Regulators Synthesis

The adjustment loop is illustrated by the diagram in Figure 3. The used regulator is a proportional-integral (PI) controller. It is simple to implement and ensures the desired performance for a best fit of its coefficients, [37].

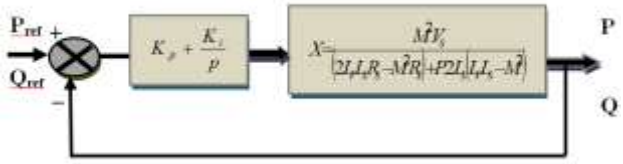

Fig. 3: Active and reactive power with PI control

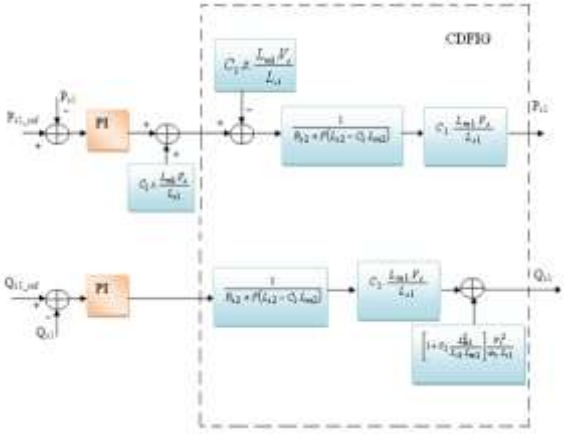

Fig. 4: Power control block diagram

Figure 4 represents the block diagram of the PI control system implementation. K_p and K_i denote the proportional and integral gains respectively, [38].

The pole compensation technique is used for their computation with a 10 ms time response specification. This constant time is fixed based on the plant dynamics and avoids transient behavior with important overshoots for lower values. The obtained gains are:

$$\frac{K_i}{K_p}=\frac{R_s\left(2.L_rL_s-M^2\right)}{2.L_s\left(L_rL_s-M^2\right)} \qquad T_r=\frac{2.L_s\left(L_rL_s-M^2\right)}{K_p.V_s.M^2} \quad (24)$$

Taking a response time: T_r=10ms, we will get:

K_p =0.0001185312; K_i =0.001842.

3.2 Proposed Fractional order MRAC Control

Adaptive control is a control technique that provides an efficient approach for automatic controller adjustment in real-time, aiming to achieve or to maintain a specified level of performance in the presence of unknown or slowly varying parameters.

The control system measures a predefined objective function of the system behavior using the input, the states, the outputs, and the known disturbances. The main concept in Model Reference Adaptive control is to make the closed-loop control system able to update the controller parameters in order to change the system response. A comparator computes the gap between the system output and the desired reference model response in real time. This error signal is used to update the control parameters. This configuration allows the parameters to converge to ideal values and thus, the plant output tracks the desired response.

In the proposed MRAC control scheme this updating law is based on a fractional order integral and aims to improve the plant behavior, [39].

3.2.1 Fractional-order Systems

The description equation of a fractional order process may be given in the frequency domain as:

$$X(s)=\frac{k}{(1+\frac{s}{p})^{\alpha}} \quad (25)$$

where,

α: fractional exponent.

p: fractional pole which is the cut frequency,

s: Laplace operator.

The literature presents a number of works that demonstrate the advantage of using fractional-order systems with their inherent good properties in dynamics performance and robustness, [40].

3.2.2 Approximation of Fractional Order Systems

The singularity function method [41] is used here to approximate the fractional order transfer functions. For fractional second order system with α a positive real number such that 0<α<1,

$$H(s)=\frac{1}{\left(\frac{s^2}{\omega^2}+2\xi\frac{s}{\omega}+1\right)^{\alpha}} \quad (26)$$

Can be expressed as:

$$H(s)=\frac{\left(\frac{s}{\omega}+1\right)\left(\frac{s}{\omega+1}\right)^{\beta}}{\left(\frac{s^2}{\omega^2}+2\mu\frac{s}{\omega}+1\right)} \quad (27)$$

with $\mu=\xi^{\alpha}$ and $\beta=1-2\alpha$, which can also be approximated by the function (19):

$$H(s)=\frac{\left(\frac{s}{\omega}+1\right)}{\left(\frac{s^2}{\omega^2}+2\alpha\frac{s}{\omega}+1\right)}\frac{\prod_{i=1}^{N-1}(1+\frac{s}{z_i})}{\prod_{i=1}^{N}(1+\frac{s}{p_i})} \quad (28)$$

3.2.3 Model Reference Adaptive Control

The difference between the plant output and the reference model one is used for the controller parameter adjustment. This can be illustrated in Figure 3.

The formula given below is used to calculate the control signal,

$$u=\varphi^T.\theta \quad (29)$$

Where φ is the regression vector representing the measured input signals *u* and output signal *y* and the input reference signal u_c. The resulting algorithm is illustrated by the block-scheme block scheme of Figure 5.

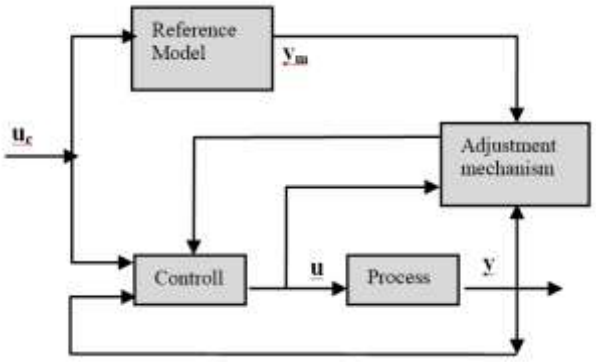

Fig. 5: Direct Model Reference Adaptive Control

3.2.4 M.I.T. Rule

The regulator in the closed loop system is supposed to have an adjustable parameter vector θ. The output is y_m of the reference model and defines the desired closed-loop behaviour, [42]. Let *e* be the gap between the closed loop system output *y* and the

model one y_m, we can adjust the parameters in a way to make:

$$J(\theta)=\frac{1}{2}e^2 \tag{30}$$

be minimized. With the aim to render J small the method is to vary parameters in the direction of negative gradient J, so:

$$\frac{d\theta}{dt}=-\gamma\frac{\partial J}{\partial\theta}=-\gamma e\frac{\partial e}{\partial\theta} \tag{31}$$

which leads to the following blocs scheme of Figure 6.

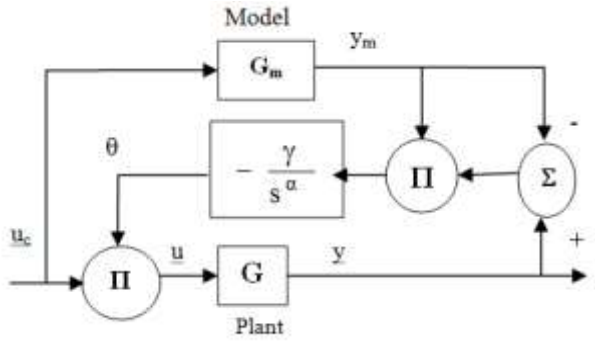

Fig. 6: Adaptation algorithm

3.2.5 Introducing Fractional Integration

There are several mathematical definitions for the integration and the fractional order derivation. These definitions always do not lead to identical results but are equivalent for a broad range of functions, [43]. Three definitions significant and largely applied and the most met are the definition of Riemann-Liouville, the definition of Caputo and the definition of Grünwald-Letnikov which is perhaps most known because of its greater aptitude for the realization of a discrete algorithm, [44].

Let $\alpha\in C$, $\Re(\alpha)>0$, $c\in R$ and f a locally integrable function defined on [c,+∞[. The αorder integral of *f,* of lower bound c is defined as:

$$I_c^{\alpha}f(t)\overset{\Delta}{=}\int_c^t\frac{(t-\tau)^{\alpha-1}}{\Gamma(\alpha)}f(\tau)d\tau \tag{32}$$

With $t\geq c$, and Γ is the Euler function. The formula (32) is called *Riemann-Liouville Integral*.
Generally, the control system is discreet, so we use a sampled approximation of (33) given by:

$$I_c^{\alpha}f(k\Delta)=\frac{\Delta}{\Gamma(\alpha)}\sum_{\tau=0}^{k-1}(k\Delta-\tau\Delta)^{\alpha-1}f(\tau\Delta) \tag{33}$$

With, Δ: Sampling Period.
In the tuning algorithm illustrated by the block scheme of Figure 4, we introduce a fractional integration of non-zero positive real order α such that: 0 <α< 2. We get the:

$$\theta=-\frac{\gamma}{s^{\alpha}}y_m(y-y_m)=-\frac{\gamma}{s^{\alpha}}y_m e \tag{34}$$

3.2.6 Application of Model Reference Adaptive Control to CDFIG Active and Reactive Power Control

The block diagram of the MRAC control of active and reactive power of the CDFIG is shown in Figure 7, by adding the parameters of the CDFIG system presented in Table 1.

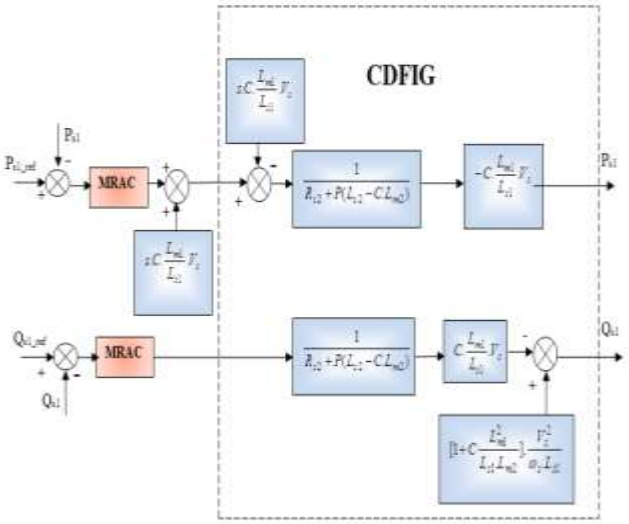

Fig. 7: MRAC of active and reactive power for CDFIG

Table 1. Characteristic parameters of the CDFIG.

Parameter	Value
V_g	*690 V*
P_1=P_2	*2* pairs of pôles.
P	*1.5* Mw
Rs1= Rs2	0.012 Ω
Rr1= Rr2	0.021Ω
Ls1= Ls2	0.0137H
Lr1= Lr2	0.0137 H
Lm1=Lm1	0.0135 H
f	50 Hz
f1=f2	0.0071 (N.m.s)/rad
J1=J2	50 Kg.m^2.

4 Results and Discussion

In this section, we will have the results of the simulation of the uncoupled control from the active and reactive powers generated doubly fed induction generator CDFIG of the wind energy, using Classical PI controller, then adaptive control

with integer reference model MRAC and fractional order model FO-MRAC, whose objective is to compare the responses of active and reactive powers compared to the references desire.

4.1 PI Controllers

The simulation results using the classical PI controller are given in Figure 8, Figure 9, Figure 10, Figure 11, Figure 12 and Figure 13.

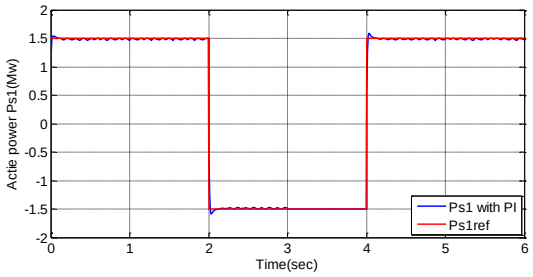

Fig. 8: CDFIG active power Ps1 for direct control with PI regulator

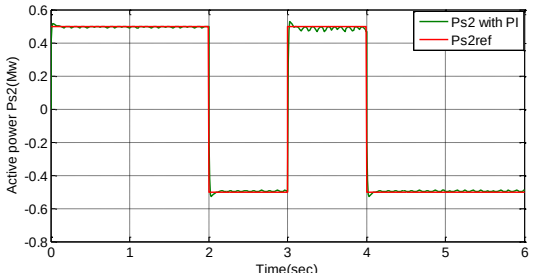

Fig. 9: CDFIG active power Ps2 for direct control with PI regulator

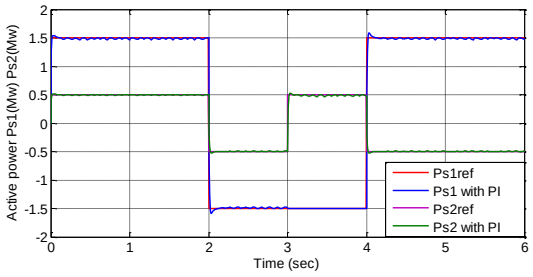

Fig. 10: CDFIG active power Ps1, Ps2 for direct control with PI regulator

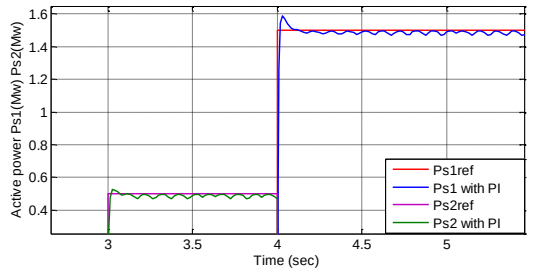

Fig. 11: Zoom of CDFIG active power Ps1, Ps2 for direct control with PI regulator

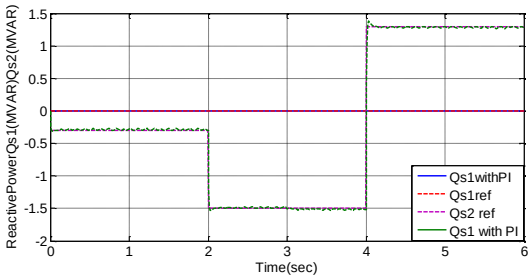

Fig. 12: CDFIG reactive power Qs1, Qs2 for direct control with regulator

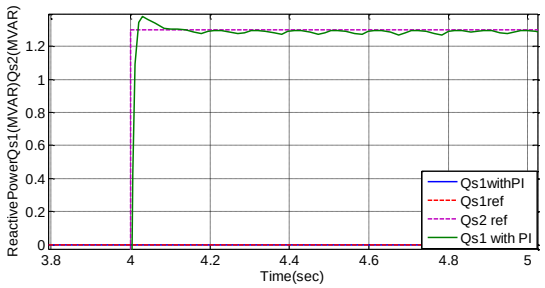

Fig. 13: Zoom of CDFIG reactive power for direct control with PI regulator

4.2 MRAC Control

4.2.1 Using an Integer Order Reference Model

The system is described using the bloc scheme of Figure 3 and the reference model has the following transfer function:

$$\mathrm{H(s)} = \frac{Y(S)}{U(S)} = \frac{8.437e05}{S+15.5} = \frac{B}{A} \qquad (35)$$

According to characteristics of the studied system, we chose the reference model as follows:

$$\mathrm{Gm(s)} = \frac{250000}{(S^2+950.S+6.4e07)^m} = \frac{Bm}{Am} \qquad (36)$$

RST Regulator parameters design (integer MRAC, m=1):

Using the equation linking the studied system and the RST configuration, we have:

$$\mathrm{A\ R + B\ S = A_r = A_0\ A_m} \qquad (37)$$

The parameters *k*, *l* and *m* represent respectively the degrees of the polynomials *R*, *S* and *T* with:

A=1 the order of denominator of system

B= 0 the order of nominator of the system

A_m= the order of denominator of the model

R= of order 1 for balance, we take:

k=degR=1 , l= degS=1 and m= degT=1.

Therefore, the vector of regulation parameters is:

$$\theta = \begin{bmatrix} r_0 & s_0 & s_1 & t_0 & t_1 \end{bmatrix}$$

$$\varphi^T = \frac{b_0}{A_0 A_m}\begin{bmatrix} U & sY & Y & -sU_c & -U_c \end{bmatrix} \quad (38)$$

Figure 14 illustrates the open-loop step response of the cascaded doubly fed generator whereas Figure 15 represents its Bode diagram.

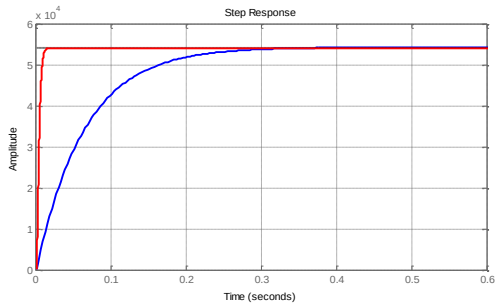

Fig. 14: Step response of the open-loop of cascaded doubly fed induction Generator power system

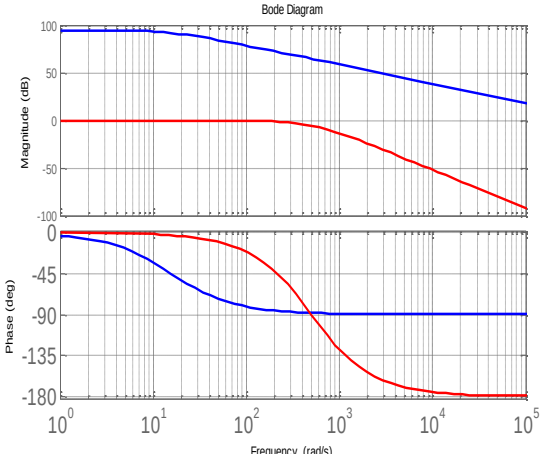

Fig. 15: Bode diagram of the open-loop of cascaded doubly fed induction Generator CDFIG power system (blue) and model (red)

4.2.2 Integer order MRAC Controller of CDFIG

Figure 16, Figure 17 and Figure 18 represent the active power output for power machine Ps1, the error signal and the control signal respectively using the integer order MRAC control.

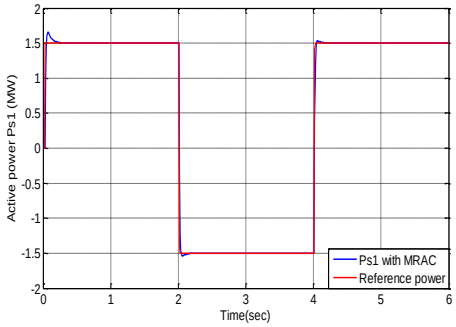

Fig. 16: Active power output control of Power machine Ps1 with integer order reference model MRAC

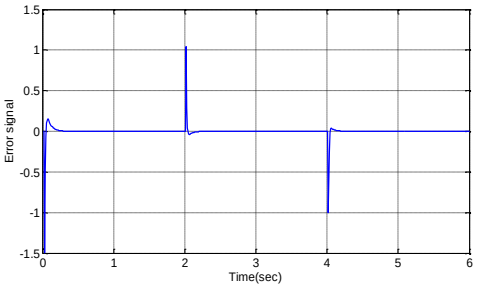

Fig. 17: Error signal with MRAC control in integer order reference model control of Power machine

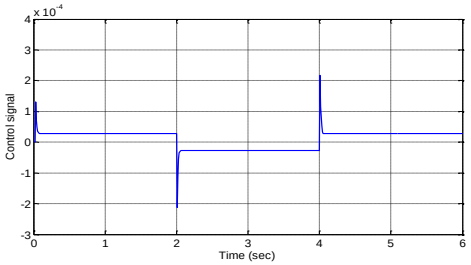

Fig. 18: Control signal with MRAC and integer order reference model control of Power machine

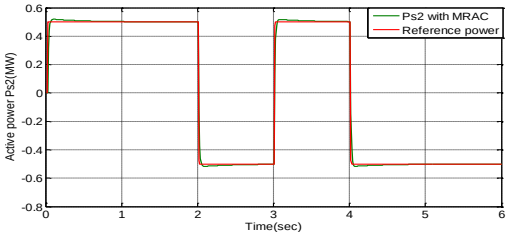

Fig. 19: Active power output control of Control Machine Ps2 with integer order reference model MRAC control

Figure 19, Figure 20 and Figure 21 represent the active power output for power machine Ps2, the error signal and the control signal respectively using the integer order MRAC control.

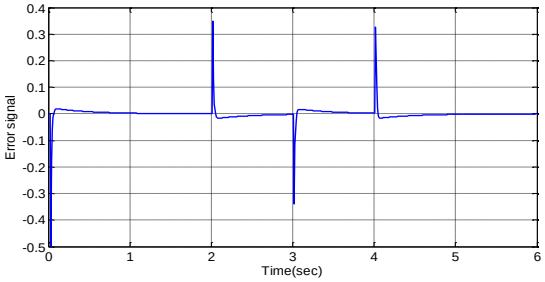

Fig. 20: Error signal with MRAC control and integer order reference model of Control Machine

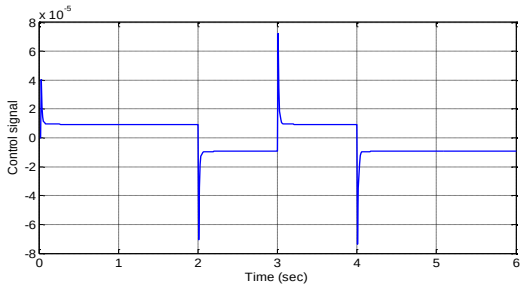

Fig. 21: Control signal with MRAC and integer order reference model of Control Machine

Figure 22 shows a comparative response of the Power Machine Ps1 and Control Machine Ps2 with integer order reference model MRAC.

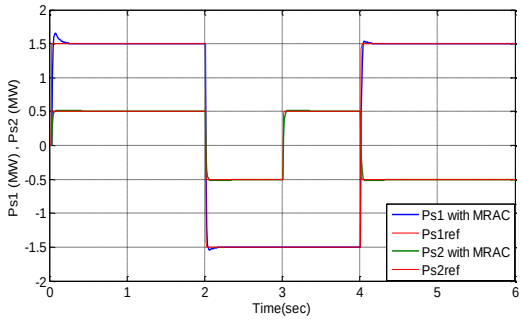

Fig. 22: Active power output of Power Machine Ps1 and Control Machine Ps2 with integer order reference model MRAC

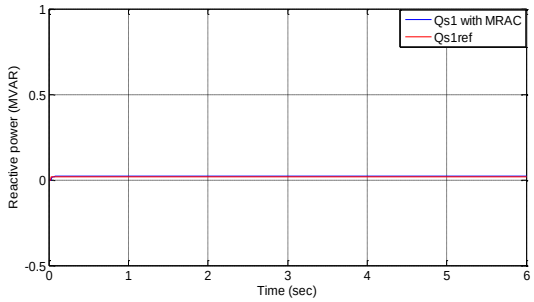

Fig. 23: Reactive power output control of Power Machine Qs1 with integer order reference model MRAC

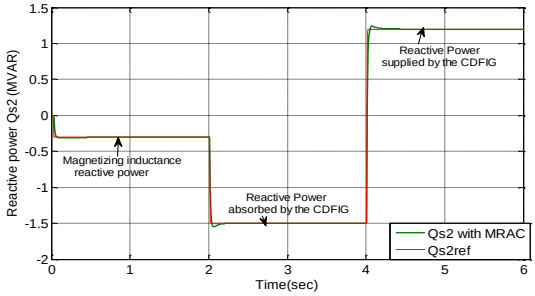

Fig. 24: Reactive power output control of Control Machine Qs2 with integer order reference model MRAC control

Figure 23 and Figure 24 represent the reactive power output for power machine Qs1 and Qs2 respectively.

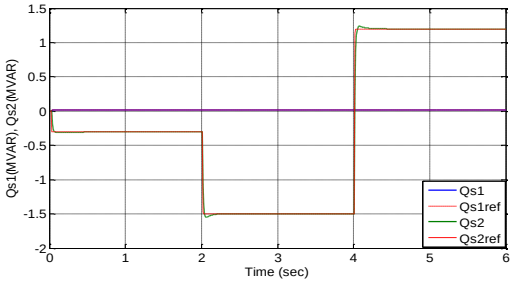

Fig. 25: Reactive power output of Power Machine Q_{s1} and Control Machine $Q_{s2}$with integer order reference model MRAC control

Figure 25 shows the responses of the power machine Qs1 and the control machine Qs2 using an integer order MRAC controller.

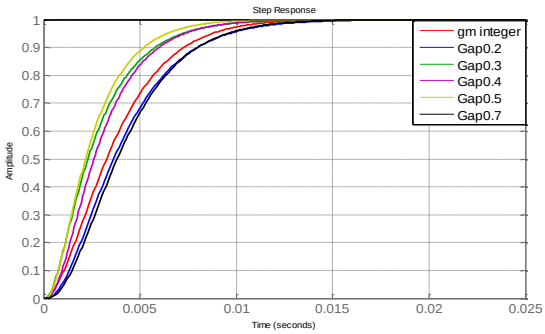

Fig. 26: Comparative step response of the integer and fractional order reference models

Figure 26 represents a comparative step response of the integer order and the fractional order reference models for different values of α.

4.3 FOMRAC Controllers Applied to CDFIG

Taking the desired reference model as a fractional order second order-like transfer function of the form (26) with α = 0.4, and using the singularity function method we obtain the approximating rational transfer function given by:

$$G_{ap0.4}(s) = \frac{0.001867s+1}{9.102e^{-13}s^4+5.196e^{-9}s^3+8.445e^{-6}s^2+0.004995s+1} \quad (39)$$

With $\xi = 0.95$, $\omega_n = 500$, $\alpha = 0.4$, $\varepsilon = 3\ dB$.

The time domain and frequency domain responses of this chosen model compared to the integer order one are illustrated in Figure 27 and Figure 28 respectively.

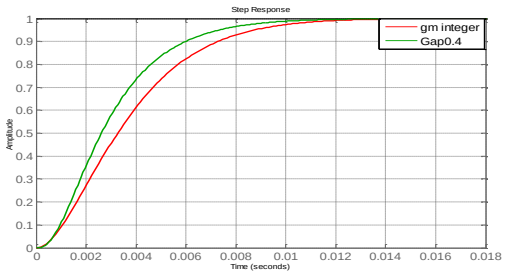

Fig. 27: Comparative step response of the integer order reference model MRAC and the fractional order reference model FOMRAC with α = 0.4

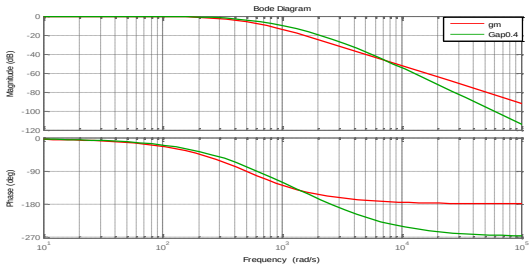

Fig. 28: Comparative bode diagram of the integer and the fractional-order reference model for α = 0.4

Applying the fractional order MRAC control scheme using the reference model (39) to the CDFIG we obtain the simulation results of Figure 29, Figure 30, Figure 31, Figure 32, Figure 33 and Figure 34.

A comparative study of these results for the MRAC and FOMRAC controllers based on the quadratic error criterion for active and reactive power of power machine (Ps1, Qs1) and control machine (Ps2, Qs2) is given in Table 2.

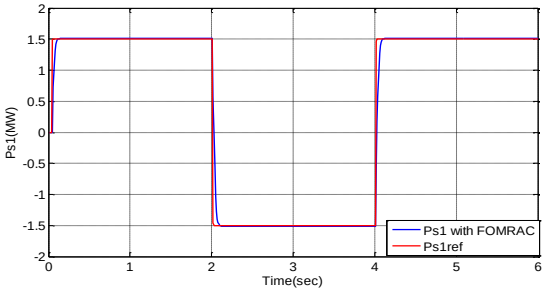

Fig. 29: Active power output of power machine $P_{s1}$with FOMRAC for α=0.4

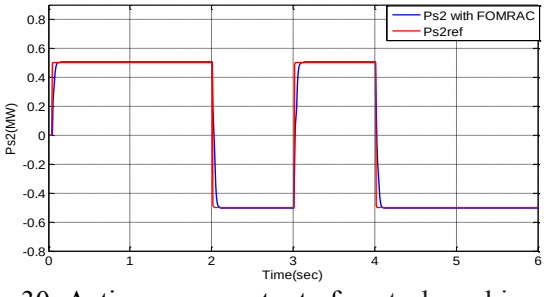

Fig. 30: Active power output of control machine $P_{s2}$with FOMRAC for α=0.4

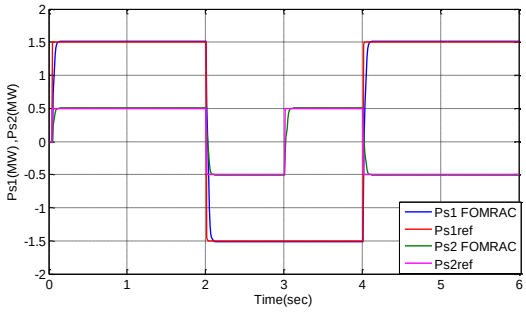

Fig. 31: Active power of Power Machine Ps1 and Control Machine Ps2 with FOMRAC for α=0.4

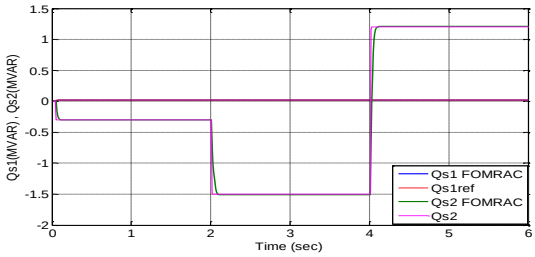

Fig. 32: Reactive power of Power Machine Qs1 and Control Machine Qs2 with FOMRAC for α=0.4

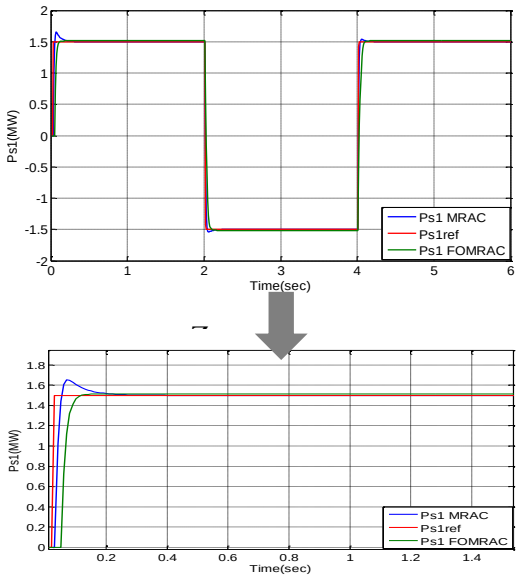

Fig. 33: Active power output comparison between MRAC and FOMRAC for α = 0.4

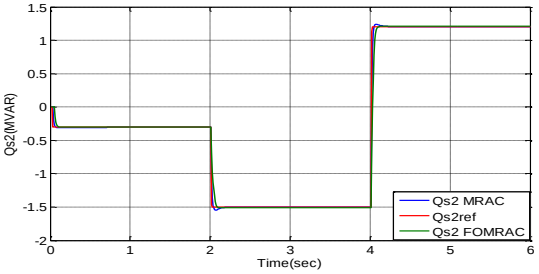

Fig. 34: Reactive power comparison between MRAC and FOMRAC for α = 0.4

Table 2. Comparative quadratic error criterion for active and reactive power of power machine (Ps1, Qs1) and control machine (Ps2, Qs2) with MRAC and FOMRAC

Active Ps and reactive power Qs	quadratic error criterion J	
	MRAC	FOMRAC
Ps1	4.8162	4.7242
Ps2	1.9413	1.8124
Qs1	0.0231	0.0175
Qs2	3.1845	3.0752

5 Discussions

Simulation results demonstrate that the proposed control strategy using FO-MRAC with a fractional order reference model is more powerful in regard to the response time and overshoot than the classical controllers with PI regulators (Figure 8, Figure 9, Figure 10, Figure 11, Figure 12 and Figure 13), or even integer order MRAC (Figure 14, Figure 15, Figure 16, Figure 17, Figure 18, Figure 19, Figure 20, Figure 21, Figure 22, Figure 23, Figure 24, Figure 15 and Figure 26).

The active and reactive power responses using PI regulators contain disturbances (see the zoom in Figure 11 and Figure 13), because the parameters of this regulator depend directly on the parameters of the machine which presents variations over time. These disturbances increase the joule effect losses of the two machines, which causes a minimization of the efficiency of the CDFIG cascade system and reduces the lifespan of the machines and the connected wind power system.

To remedy this drawback we proposed and studied the control of the cascade of the two DFIG machines by the use of the adaptive control with integer reference model MRAC and fractional FOMRAC, where the comparison between these two techniques is illustrated in Figure 33 and Figure 34. They prove that the FO-MRAC control with fractional-order reference gives better performance than the integer order MRAC because the responses of active and reactive power follow perfectly the suggested references.

Also, Table 2 presents the active and reactive power output comparison between the integer order reference model MRAC and fractional order reference model FOMRAC. It confirms that the tracking error obtained for FO-MRAC is smaller than that obtained for the MRAC in active and reactive power control.

6 Conclusion

The idea to install a cascade of two DFIG in the chains of wind conversion is a promising solution for the stage with the disadvantage of the system ring-brushes when only one DFIG is envisaged. The order uncoupled from the powers proved to be powerful, allowing even an operation with a unit reactivity power coefficient.

Through the study carried out under wind operation, one manages to control stator 1 through stator 2.Stator 1 product always of energy activates while following the reference.

Stator 2 product or consumes active and reactive energy while following the speed of the wind. In hyposynchronous, it consumes energy and in hyper-synchronous it provides to the network energy, two energies are varies independently one of the other, which, is noticed that the variation of active energy does not influence the pace of the reactive energy which presents a value depending on magnetizing of the magnetic circuit fixes then it takes a fixed and null value in permanent mode.

Our work is a continuation and additional confirmation of the effectiveness and the good performances obtained by the use of the adaptive fractional order control of active and reactive power in wind energy systems comparatively with classical control using PI controller; where we have started this paper with modelling of the cascaded doubly fed induction generator CDFIG, then we presented the system control with classical PI regulator, after that we proposed an adaptive control scheme with both conventional MRAC and fractional order model reference FOMRAC configurations. Then, we performed the analysis, design, and numerical implementation of these control actions with success to the cascaded DFIG system.

These techniques are more powerful with regard to the error, response time, and overshoot than the classical control with PI regulators which are the most commonly used, however, selection of controller gains is not easy and is usually subject to continuous adjustment. We conclude that the FO-MRACadaptive controller is able to optimize the energy transfers in wind energy plants.

Parameters of CDFIG

The used machines are identical:
P=1.5 MW ; Vg=690V
P1=P2=2; f1=f2= 0.0071N.m.s/rad;
J1=J2=50 Kg.m^2.
Rs1= Rs2= 0.012Ω ; Rr1= Rr2= 0.021Ω ;
Ls1= Ls2= 0.0137H ; Lr1= Lr2= 0.0137 H ;
Lm1=Lm1= 0.0135H;

Nomenclatures:

CDFIG	Cascaded Doubly-Fed Induction Generator
DFIG	Doubly-Fed Induction Generator
$\mathbf{P_i}$	Active power
$\mathbf{Q_i}$	Reactive power
I_{si} $(i=1,2)$	Stator currents
I_{dsi} $(i=1,2)$	Stator currents on the axis d
I_{qsi} $(i=1,2)$	Stator currents on the axis q
I_{ar}, i_{br}, i_{cr} :	Rotor currents
$I_{.dr}$	Rotor current on the axis d
I_{qr}	rotor current on the axis q
s_1	Slip of the 1st machine.
s_2	Slip of the 2nd machine.
s	Slip of the cascade of two machines.
C_e	Electromagnetic couple
C_r	Resistive torque
J	Inertia of the revolving masses
f	Coefficient of viscous friction
K_p ;	Constant proportional of the regulator
K_i ;	Constant integral of the regulator

References:

[1] Oustaloup A, Sabatier J, Lanusse P, Malti R, Melchior P, Moreau X, Moze M,An overview of the CRONE approach in system analysis, modeling and identification, observation and control, *IFAC Proceedings*, Volumes, Vol. 41, No. 2, 2008, pp. 14254-14265. DOI: 10.3182/20080706-5-KR-1001.02416.

[2] Monje CA, Chen YQ, Vinagre BM, Xue D, Feliu V. *Fractional-order Systems and Controls: Fundamentals and Applications*, Springer-Verlag, London, 2010. DOI: 10.1007/978-1-84996-335-0.

[3] Sutha S, Lakshmi P, Sankaranarayanan S. Fractional-order sliding mode controller design for a modified quadruple tank process via multi-level switching, *Computers and Electrical Engineering*, Vol. 45, 2015, pp. 10–21. DOI: 10.1016/j.compeleceng.2015.04.012.

[4] Zamani M, Karimi-Ghartemani M, Sadati N, Parniani M, Design of a fractional order PID controller for an AVR using particle swarm optimization, *Control Engineering Practice*, Vol. 17, 2009, pp. 1380–1387. DOI: 10.1016/j.conengprac.2009.07.005.

[5] Gupta DK, Dei G, Soni AK, Jha AV, Appasani B, Bizon N, Srinivasulu A, Nsengiyumva P. Fractional order PID controller for load frequency control in a deregulated hybrid power system using Aquila Optimization, *Results in Engineering*, Vol. 23, 2024, 102442. DOI: 10.1016/j.rineng.2024.102442.

[6] Raj U, Shankar R. Optimally enhanced fractional-order cascaded integral derivative tilt controller for improved load frequency control incorporating renewable energy sources and electric vehicle. *Soft Computing*, Vol. 27, 2023, pp. 15247–15267. DOI: 10.1007/s00500-023-07933-3.

[7] Alilou M, Azami H, Oshnoei A, Mohammadi-Ivatloo B, Teodorescu R. Fractional-Order Control Techniques for Renewable Energy and Energy-Storage-Integrated Power Systems: A Review. *Fractal and Fractional*, Vol. 7, No. 5, 2023, 391. DOI: 10.3390/fractalfract7050391.

[8] Najari M, Balochian S, Adaptive Predictive Control of Fractional Order Chaotic Systems, *Electrica*, Vol. 24, No. 1, 2024, pp. 3-11. DOI: 10.5152/electrica.2024.23047.

[9] Vinagre BM, Petras I, Podlubny I, Chen YQ. Using fractional order adjustment rules and fractional order reference models in model-reference adaptive control. *Nonlinear Dynamics*, Vol. 29, No. 1–4, 2002, pp. 269–279. DOI: 10.1023/A:1016504620249.

[10] Benchaita H, Ladaci S. Fractional adaptive SMC fault tolerant control against actuator failures for wing rock supervision, *Aerospace Science and Technology*, Vol. 114, 2021, 106745. DOI: 10.1016/j.ast.2021.106745.

[11] Perumal V, Kannan SK, Balamurugan CR. Grid Mode Selection Scheme based on a Novel Fractional Order Proportional Resonant Controller for Hybrid Renewable Energy Resources, *Electric Power Components and Systems*, Vol. 51, No. 16, 2023, pp. 1710-1729. DOI: 10.1080/15325008.2023.2202674.

[12] Yan S-R, Dai Y, Shakibjoo AD, Zhu L, Taghizadeh S, Ghaderpour E, Mohammadzadeh A. A fractional-order multiple-model type-2 fuzzy control for interconnected power systems incorporating renewable energies and demand response, *Energy Reports*, Vol. 12, 2024, pp. 187-196. DOI: 10.1016/j.egyr.2024.06.018.

[13] Varga B, Tar JK, Horváth R, Fractional order inspired iterative adaptive control, *Robotica*, Vol. 42, No. 2, 2024, pp. 482-509. DOI: 10.1017/S0263574723001595.

[14] Aburakhis M, Ordóñez R. Generalization of Direct Adaptive Control Using Fractional Calculus Applied to Nonlinear Systems. *Journal of Control, Automation and Electrical Systems,* Vol. 35, 2024, pp. 428–439. DOI: 10.1007/s40313-024-01082-0.

[15] Saleem O, Ahmad KR, Iqbal J, Fuzzy-Augmented Model Reference Adaptive PID Control Law Design for Robust Voltage Regulation in DC–DC Buck Converters, *Mathematics*, Vol. 12, No. 12, 2024,1893. DOI: 10.3390/math12121893.

[16] Djebbri S, Ladaci S, Metatla A, Balaska H. Fractional-order model reference adaptive control of a multi-source renewable energy system with coupled DC/DC converters power compensation, *Energy Systems*, Vol. 11, 2020, pp. 315–355. DOI: 10.1007/s12667-018-0317-5.

[17] Djebbri S, Balaska H, Ladaci S. Robust MRAC-based adaptive control of a Doubly Fed Induction Generator (DFIG) in a Wind energy system using a fractional order Integrator, *Algerian Journal of Signals and Systems*, Vol. 5, No. 1, 2020, pp. 40–46. DOI: 10.51485/ajss.v5i1.94.

[18] Lv Z-X, Liao J. Fractional-Order Model-Free Adaptive Control with High Order Estimation, *Mathematics*, Vol. 12, No. 5, 2024, 784. DOI: 10.3390/math12050784.

[19] Tian T, Hou X, Yan F, A new output feedback adaptive control method for fractional order systems with inaccessible state, *Chinese Journal of Physics*, Vol. 90,2024, pp. 1046-1056. DOI: 10.1016/j.cjph.2024.04.004.

[20] Aguila-Camacho N, Duarte-Mermoud MA. Combined Fractional Adaptive Control, *IFAC-PapersOnLine*, Vol. 50, No. 1, 2017, pp. 8586-8591. DOI: 10.1016/j.ifacol.2017.08.1423.

[21] Yan F, Hou X, Tian T. Fractional-Order Multivariable Adaptive Control Based on a Nonlinear Scalar Update Law, *Mathematics*, Vol. 10, No. 18, 2022, 3385. DOI: 10.3390/math10183385.

[22] Wan Y, Zhang H, French M, Adjustable Fractional Order Adaptive Control on Single-Delay Regenerative Machining Chatter, *Journal of Fractional Calculus and Applications*, Vol. 6, No. 1, 2015, pp. 185-207. DOI: https://dx.doi.org/10.21608/jfca.2015.306005.

[23] Zhang L. Wind Energy Development: History and Current Status, *Wind, Water and Fire*. 2021, pp. 1-6. DOI: 10.1142/11985.

[24] Hannan MA, Al-Shetwi AQ, Mollik MS, Ker PJ, Mannan M, Mansor M, Al-Masri HMK, Mahlia TMI. Wind Energy Conversions, Controls, and Applications: A Review for Sustainable Technologies and Directions. *Sustainability*, Vol. 15, 2023, 3986. DOI: 10.3390/su15053986.

[25] Dauksha G, Iwanski G. Indirect Power Control of a Cascaded Brushless Doubly-Fed Induction Generator Operating with Unbalanced Power Grid, *2021 IEEE 19th International Power Electronics and Motion Control Conference (PEMC)*, Gliwice, Poland, 25-29 April 2021. DOI: 10.1109/PEMC48073.2021.9432628.

[26] Boukettaya G, Naifar O, Ouali A, A vector control of a cascaded doubly fed induction generator for a wind energy conversion system. *2014 IEEE 11th International Multi-Conference on Systems, Signals & Devices (SSD14)*, 11-14 February 2014. DOI: 10.1109/SSD.2014.6808821.

[27] Vasconcelos C, Stephan R, Ferreira AC, Study of The Cascaded Doubly Fed Induction Machine Dynamics Under Vector Control, *Eletrônica de Potência*, Vol. 23, No. 1, 2018, pp. 39-46. DOI: 10.18618/REP.2018.1.2719.

[28] Adamowicz M, Strzelecki R, Cascaded doubly fed induction generator for mini and micro power plants connected to grid, *2008 13th International Power Electronics and Motion Control Conference*, Poznan, Poland, 01-03 September 2008. DOI: 10.1109/EPEPEMC.2008.4635516.

[29] Din Z, Zhang J, Zhao J, Jiang Y. Doubly Fed Induction Generator with Cascade Converter for Improving Dynamic Performances, *2018 IEEE Energy Conversion Congress and Exposition (ECCE)*, Portland, OR, USA, 23-27 September 2018. DOI: 10.1109/ECCE.2018.8558069.

[30] Carlson R, Voltolini H, Runcos F, Peng PK, A performance comparison between brush and brushless doubly fed asynchronous generators for wind power systems, *Renewable Energy and Power Quality Journal*, Vol. 1, No. 4, 2006, pp. 258-262. DOI: 10.24084/repqj04.405.

[31] El Achkar M, Mbayed R, Salloum G, Patin N, Monmasson E. Voltage Control of a Stand-Alone Cascaded Doubly Fed Induction Generator, *IEEE Transactions on Industrial Electronics*, Vol. 66, No. 1, 2019, pp. 762-771. DOI: 10.1109/TIE.2018.2856186.

[32] Sadeghi R, Madani SM, Agha-kashkooli M-R, Ataei M. Reduced-order model of cascaded doubly fed induction generator for aircraft starter/generator, *IET Electric Power Applications*, Vol. 12, No. 6, 2018, pp. 757-766. DOI: 10.1049/iet-epa.2017.0579.

[33] Padamata AP, Rao GS. Modelling of Variable Speed Wind Turbine Connected DFIG: 250KW, *WSEAS Transactions on Power Systems*, Vol. 18, 2023, pp. 426-435. DOI: https://doi.org/10.37394/232016.2023.18.42.

[34] Louze L, Nemmour AL, Khezzar A, Hacil ME, Boucherma M. Cascade sliding mode controller for self-excited induction generator, *Revue des Energies Renouvelables*, Vol. 12, No. 4, 2009, pp. 617-626.

[35] Maafa A, Mellah H, Ghedamsi K, Aouzellag D. 2022. Improvement of Sliding Mode Control Strategy Founded on Cascaded Doubly Fed Induction Generator Powered by a Matrix Converter. *Engineering, Technology & Applied Science Research*, Vol. 12, No. 5, 2022, pp. 9217–9223. DOI: 10.48084/etasr.5166.

[36] Dauksha G, Górski D, Iwański G. State-feedback control of a grid-tied cascaded brushless doubly-fed induction machine, *Electric Power Systems Research*, Vol. 228, 2024, 110043. DOI: 10.1016/j.epsr.2023.110043.

[37] Hete RR, Shrivastava T, Dash R, Anupallavi L, Fathima M, Reddy KJ, Dhanamjayalu C, Mohammad F & Khan B. Design and development of PI controller for DFIG grid integration using neural tuning method ensembled with dense plexus terminals. *Scientific Reports*, Vol. 14, 7916, 2024, DOI: 10.1038/s41598-024-56904-7.

[38] Nguyen DD, Than NH, Hoang DT. The cascade methods of doubly-fed induction machine for generator system, *International Journal of Power Electronics and Drive Systems (IJPEDS)*, Vol. 12, No. 1, 2021, pp. 112-120. DOI: 10.11591/ijpeds.v12.i1.pp112-120.

[39] Ladaci S, Loiseau JJ, Charef A. Using fractional order filter in adaptive control of noisy plants, *International Conference on Advances in Mechanical Engineering And Mechanics, ICAMEM 2006*, Hammamet, Tunisia.

[40] Juchem J, Muresan C, De Keyser R, Ionescu C-M, Robust fractional-order auto-tuning for highly-coupled MIMO systems, *Heliyon*, Vol. 5, No. 7, 2019, e02154. DOI: 10.1016/j.heliyon.2019.e02154.

[41] Charef A, Sun HH, Tsao YY, Onaral B. Fractal system as represented by singularity function, *IEEE Transactions on automatic control*, Vol. 37, No. 9, 1992, pp. 1465-1470. DOI: 10.1109/9.159595.

[42] Rothe J, Zevering J, Strohmeier M, Montenegro S, A Modified Model Reference Adaptive Controller (M-MRAC) Using an Updated MIT-Rule for the Altitude of a UAV, *Electronics*, Vol. 9, No. 7, 2020, 1104. DOI: 10.3390/electronics9071104.

[43] Gutiérrez RE, Rosário JM, Machado JT, Fractional Order Calculus: Basic Concepts and Engineering Applications, *Mathematical Problems in Engineering*, 2010, DOI: 10.1155/2010/375858.

[44] Sarkar DU, Prakash T, Singh SN, Fractional Order PID-PSS Design using Hybrid Deep Learning Approach for Damping Power System Oscillations, *IEEE Transactions on Power Systems*, 2024, 1-13, DOI: 10.1109/TPWRS.2024.3416753.

Contribution of Individual Authors to the Creation of a Scientific Article (Ghostwriting Policy)

- Sihem Djebbri, carried out theinvestigation and simulation,the implementation of the proposed controllers, Validation, and Writing the original draft.
- Samir Ladaci contributed to the Conceptualization, Investigation, Methodology, Supervision, and Writing - review & editing.

Sources of Funding for Research Presented in a Scientific Article or Scientific Article Itself

No funding was received for conducting this study.

Conflict of Interest

The authors have no conflicts of interest to declare.